Received: 18 September 2023 | Revised: 7 February 2024 | Accepted: 26 February 2024

IET Radar, Sonar & Navigation

DOI: 10.1049/rsn2.12555

The Institution of Engineering and Technology WILEY

ORIGINAL RESEARCH

Sequence optimisation for compressed sensing CDMA MIMO radar via mutual coherence minimisation

Saravanan Nagesh[1] | María A. González-Huici[1] | Andreas Bathelt[1] | Miguel Heredia Conde[2] | Joachim Ender[1,2]

[1]Department of Signal Processing and Algorithms, Industrial High Frequency Systems (IHS), Fraunhofer FHR, Wachtberg, Germany

[2]Center for Sensor Systems (ZESS), Universität Siegen, Siegen, Germany

Correspondence

Saravanan Nagesh, 0.09, Villip2, Siebengebirgsblick 26, 53343 Wachtberg, Germany.
Email: saravanan.nagesh@fhr.fraunhofer.de

Funding information

HORIZON EUROPE Marie Sklodowska-Curie Actions, Grant/Award Number: 860370

Abstract

The authors focus on the waveform design for Code Division Multiple Access Multiple Input Multiple Output (CDMA-MIMO) radar systems, with a specific emphasis on Compressed Sensing (CS) based target estimation. The selection of an appropriate waveform is a critical determinant in the effectiveness of estimation algorithms. Recent studies show the possibilities of optimising waveform parameters to improve the efficiency of CS based estimation. The authors introduce an optimisation framework designed to modify the phase components of code sequences used in CS-CDMA MIMO radar systems. The objective of this optimisation is to minimise the l_∞ norm of off-diagonal elements within the Gramian matrix of the underlying sensing matrix, focusing on phase modulation of the waveform. Solving this optimisation problem requires dealing with a non-convex, combinatorial and non-linear scenario. Simulated Annealing is employed as the solution technique. To assess the effectiveness of the proposed optimisation approach, the resulting optimised sequence is rigorously compared against well-established Hadamard and Gold sequences across various performance metrics. These metrics encompass correlation properties, ambiguity function behaviour, recovery percentage and recovery error. The study demonstrates that the generated poly-phase sequences outperform existing sequences, leading to significantly improved target reconstruction results in the context of CDMA-MIMO radar systems with CS-based estimation.

KEYWORDS

compressed sensing, MIMO radar, phase modulation, radar waveforms

1 | INTRODUCTION

The selection of a radar waveform is crucial for how well a radar system performs. It is a critical decision that involves balancing numerous important factors, with a key consideration being the customisation of the waveform for specific applications, such as military surveillance, weather tracking or self-driving cars. Distinct radar waveforms offer varying degrees of proficiency in range resolution, target discrimination, and clutter attenuation, each of which constitutes fundamental facets of radar system effectiveness. Furthermore, the system's competence in accurately detecting and tracking targets, averting interference and maintaining operational efficacy in diverse environmental conditions is profoundly influenced by various parameters, including pulse duration, modulation strategies and frequency selection. The intricate process of waveform design, thus, demands judicious analysis and thoughtful trade-offs to optimise the overarching performance of the radar system in accordance with its designated mission objectives [1].

When concerning MIMO radar systems, a variety of waveforms are employed to optimise their performance across a spectrum of applications. These waveforms can encompass traditional pulse-Doppler waveforms, such as linear frequency

modulation and constant-frequency continuous-wave (CW) signals, as well as more advanced waveforms, including orthogonal frequency-division multiplexing and phased-coded waveforms. One of the key requirements when concerning waveforms for MIMO radar systems is transmit orthogonality [2]. Transmit orthogonality refers to a condition where the waveforms or signals transmitted from different antennas or transmitters are orthogonal to each other. Orthogonality signifies that the signals are statistically independent and do not interfere with each other when received by the receiver. In general, transmit orthogonality for MIMO radars can be achieved via Time-Division Multiple Access, Doppler-Division Multiple Access, Code-Division Multiple Access (CDMA), and Frequency-Division Multiple Access. For interested readers, a comprehensive exploration of the merits and drawbacks of the various transmission strategies for MIMO radars, is available in ref. [3].

MIMO radar transmission strategies face two principal challenges, sidelobes and ambiguities. Sidelobes result from signal processing methods applied during reception, such as matched filtering, while ambiguities, often known as grating lobes, are rooted in the inherent characteristics of the waveform or antenna array configuration. Resolving ambiguities proves difficult since they closely resemble genuine target responses, making them indistinguishable even with advanced reception algorithms. Sidelobes, in contrast, are weaker lobes or peaks in the radar signal's radiation pattern, typically surrounding the main lobe, which contains the primary signal of interest. They can lead to issues, such as interference, false targets, reduced sensitivity and masking but are comparatively more manageable. When comparing sidelobes with ambiguities, we have the potential to address sidelobes using advanced signal processing techniques, such as Sparse Signal Processing (SSP). Therefore, an optimal strategy for MIMO radars would involve designing waveforms that trade sidelobes for ambiguities on the transmit side and implementing intelligent processing algorithms to mitigate sidelobes on the receiver side [4]. One such promising approach is to combine sparse reconstruction algorithms with CDMA transmission.

CDMA MIMO radar systems represent a transformative advancement in the field of radar technology. They combine the principles of CDMA, originally devised for communication applications, with the spatial diversity and beamforming capabilities of MIMO radar. Transmit orthogonality for CDMA MIMO radar is achieved through the utilisation of unique orthogonal codes, enabling multiple transmit elements to coexist and operate concurrently within the same frequency band without introducing interference within the same system [5]. These orthogonal codes, which modulate the phase component of the waveform, are commonly referred to as phase-modulated waveforms. In this study, our focus is explicitly on continuous wave radars; hence, we refer to the waveforms used for CDMA MIMO radars as Phase Modulated Continuous Waveforms (PMCW).

Numerous studies have explored PMCW waveforms for MIMO radars [6–9] and performance evaluations of the system have been extensively conducted [5, 10–12]. Recent research studies [13] have delved into the use of sequences, such as Gold, Kasami and m-sequence as potential candidates for PMCW MIMO radars. These studies have also investigated the impact of the choice of code and its parameters on Doppler tolerance. Building upon the foundational concepts presented in refs. [5, 13], ref. [14] introduced an innovative PC-FMCW MIMO radar architecture that incorporates a dechirping and decoding reception strategy to maintain a reduced intermediate signal bandwidth, thereby addressing existing limitations in contemporary radar solutions. In contrast to other studies that focus on utilising existing sequences, the authors in ref. [15] have proposed several novel cyclic algorithms, specifically CAN, WeCAN and CAD, designed for synthesising unimodular sequence sets suitable for phase modulation within a MIMO radar waveform. While there has been research concentrated on the development of codes with low Integrated Sidelobe Levels (ISLs) [16], it is noteworthy that CDMA MIMO radar systems can still present challenges, particularly in practical scenarios where they may inadvertently mask targets. Moreover, these systems often entail heightened computational requirements due to the concurrent operation of multiple channels, prompting an exploration into the application of Compressed Sensing (CS) techniques as a potential solution for mitigating these issues.

The introduction of CS to radar systems by Richard Baraniuk and Philippe Steeghs in ref. [17], marked a groundbreaking advancement in the realm of radar signal processing. This innovative approach showcased the feasibility of extracting target properties from sparse-range Doppler scenes, even with a limited number of measurements, thereby significantly enhancing radar signal processing efficiency. Subsequently, the field witnessed a multitude of contributions to the application of Compressed Sensing in radar (CSR) [18–23]. An area of particular interest lies in the endeavour to enhance the reconstruction efficiency of CS algorithms, a goal that can be realised through the careful design of waveforms characterised by a desirable level of incoherence. Herman and Strohmer introduced this fundamental concept in ref. [18], elucidating how waveform modification can enhance the precise recovery of sparse targets sampled at sub-Nyquist conditions. In a related context, a low-complexity algorithm for optimising transmission waveforms, specifically tailored for imaging extended targets utilising a 'compressively sampled ultra-wideband radar', was proposed in ref. [24] and further elaborated upon in ref. [23]. Enterzari and Rashidi presented a novel algorithm aimed at waveform design by optimising the coherence properties of the sensing matrix in ref. [25]. Additionally, in ref. [26], efficient approaches for waveform optimisation were proposed for both single-pulse and pulse-train scenarios. Lastly, in ref. [27], researchers explored the cognitive capabilities of CSR by suggesting that transmission waveforms and sensing matrices can be adaptively updated based on feedback from the recovery algorithm, thereby enabling dynamic optimisation driven by real-time target scene information.

The integration of sparse reconstruction algorithms with CDMA transmission offers a robust solution for achieving

simultaneous transmission across all channels and reconstructing sparse or compressible signals from undersampled measurements. Leveraging the inherent sparsity within target scenes, SSP algorithms excel at discriminating genuine target responses from sidelobes, effectively mitigating undesirable sidelobe artefacts [28]. Consequently, this integration enhances the target detection prowess of CDMA MIMO radars, all while keeping sidelobe levels in the radar beam pattern at an efficient/acceptable computational load.

Waveform design, particularly to enhance CS reconstruction performance, presents a promising avenue for active research in the realm of CS-based CDMA MIMO radar [4]. The majority of approaches to waveform design for Compressive Sensing Radar (CSR) focus on minimising the Mutual Coherence (MC) of the sensing matrix by optimising transmit waveform properties. Typically, this involves introducing incoherence into the sensing matrix through a random phase component between successive regularly transmitted pulses (as discussed in ref. [29]) or employing an irregular pulse transmission scheme in which only a subset of uniformly spaced pulses is transmitted (as mentioned in ref. [30]). However, there have been relatively few studies dedicated to optimising waveforms by adjusting their parameters within each pulse or during the fast-time (intrapulse interval). Building on our initial analysis in ref. [31], we explored the influence of different code sequences on CS reconstruction performance, laying the groundwork for this article.

In this study, we present a methodology for designing sequences customised for CDMA MIMO radar systems with the goal of achieving transmit orthogonality in fast time. The optimisation problem is formulated as the minimisation of $||\mathbf{G} - \mathbf{I}||_\infty$, with the Gram matrix $\mathbf{G}$ derived from the normalised-column sensing matrix $\hat{\boldsymbol{A}}$. The individual phase components transmitted across each transmit element are considered as optimisation parameters. The outcome of this methodology yields a family of poly-phase sequences with excellent correlation properties, an enhanced Ambiguity function (AF) response and the introduction of pronounced incoherence within the sensing matrix. Consequently, the resultant sensing matrix enhances the performance of SSP reconstruction algorithms, resulting in the reduction of receiver errors and an increase in success rates.

This paper is organised as follows. Section 2 describes the CS CDMA MIMO radar signal model. Next, Section 3 presents the formulation of the optimisation methodology. In addition, Section 4 presents the simulation results. Finally, Section 5 summarises the study's conclusions and findings.

1.1 | Notations

We use boldface lowercase for vectors (**a**) and uppercase for matrices (**A**). The transpose, Hermitian, and complex conjugate operators are denoted by symbols $(.)^{\boldsymbol{T}}$, $(.)^{\boldsymbol{H}}$, and $(.)^*$, respectively. $\mathbb{C}^{\boldsymbol{N\,X\,M}}$ is the set of $N\,X\,M$ complex matrices. diag(**a**) indicates the diagonal matrix formed by the components of vector (**a**) along the main diagonal. det(.) represents the matrix determinant, and tr(.) is the matrix trace operator. Additionally, $|\boldsymbol{A}|_0$ denotes the number of non-zero entries of the matrix **A**, $|\boldsymbol{A}|_\infty$ is the largest value of **A**, and $|\boldsymbol{A}|_F$ and $|\boldsymbol{a}|_2$ are the Euclidean norms for matrices and vectors, respectively. If **a** and **b** are two vectors, then $\langle \boldsymbol{a},\boldsymbol{b}\rangle$ is the inner product between **a** and **b** (i.e. $\langle \boldsymbol{a},\boldsymbol{b}\rangle = \boldsymbol{b}^{\boldsymbol{H}}\boldsymbol{a}$). $\boldsymbol{\lambda_{max}}(\boldsymbol{A})$ and $\boldsymbol{\lambda_{min}}(\boldsymbol{A})$ represent the maximum and minimum eigenvalues of **A**, defined only for $N = M$, respectively.

2 | SIGNAL MODEL

Our analysis pertains to a MIMO radar system that utilises N_T transmit antennas and N_R receive antennas. It is assumed that the distance between the elements is small enough to ensure a complete correlation of the radar echo from a particular scatterer across the array, implying a coherent propagation scenario. We assume a monostatic radar configuration for transmit and receive arrays (collocated MIMO) and far field. Let the receiver and transmitter array characteristics be described by their respective array manifolds as, $\boldsymbol{a_R}(\beta)$ and $\boldsymbol{a_T}(\beta)$, where $\beta = \cos(\theta)$, is the direction of arrival. We assume a linear array and a 2D geometry for the target scenario. For convenience, we formulate the analysis in terms of delay τ instead of range r. There is no loss of generality as delay and range are related by $\tau = 2r/c$, with c denoting the speed of light. All notions for Doppler have been ignored, as the focus of this study is limited to fast time (single period); hence, we concentrate only on the delay-azimuth domain.

Consider each *ith* transmit element to radiate a single complex envelope modulated with a unique sequence of length L. Let the time period of each bit be T_c and its corresponding bandwidth B_c. The transmit signal model is given by the following equation:

$$s_i(t) = \sum_{l=0}^{L-1} W_{il}\,u(t - lT_c) \tag{1}$$

where, W_{il} represents the *lth* phase component radiated from the *ith* transmitter and $u(t)$ is an elementary waveform (such as a rectangular pulse or continuous sine wave), with a period $T = LT_c$. The generic notation for all N_T transmit elements is given by $\boldsymbol{s}(t) = \boldsymbol{W}\boldsymbol{u}(t)$.

Consider the signal model for transmit and receiver antennas given by the following equation:

$$\boldsymbol{a_T}(\beta) = e^{\iota 2k_0 i \boldsymbol{d_T}\beta};\ \forall i \in [0, N_T - 1] \tag{2}$$

$$\boldsymbol{a_R}(\beta) = e^{\iota 2k_0 j \boldsymbol{d_R}\beta};\ \forall j \in [0, N_R - 1]$$

where $\boldsymbol{d_T}$ and $\boldsymbol{d_R}$ are spacing between the transmit and receive elements, and k_0 denotes the wavenumber relative to the carrier frequency. By choosing $\boldsymbol{d_T} = N_R\lambda/2$ and $\boldsymbol{d_R} = \lambda/2$ yields a uniformly spaced virtual array $\lambda/2$ spacing. The aperture of the virtual array is $(N_T N_R - 1)\lambda/2$ and is free of grating lobes.

Next, consider the i^{th} transmit antenna to radiate a coded signal as in Equation (1). Let the signals reflected by a target with unit reflectivity present at delay τ and azimuth β, captured by the j^{th} receiver, be given by the following equation:

$$y_j(t) = \sum_{i=1}^{N_T} e^{-\iota 2\pi c\lambda^{-1}\left(t-d_{i,j}(t)/c\right)} s_i\left(t - d_{i,j}(t)/c\right) \tag{3}$$

where, c denotes the speed of light and $d_{i,j}$ is the distance travelled by the transmitted signal from transmitter ith to receiver jth, at instance t, and is given by the following equation:

$$d_{i,j}(t) = \tau c + \beta d_T(i-1) + \beta d_R(j-1) \tag{4}$$

Post demodulation and considering far field assumptions, the received base-band signal at the jth receiver is approximated as follows:

$$y_j(t) \approx e^{\iota 2\pi\lambda^{-1}c\tau} e^{\iota 2\pi\beta d_R(j-1)\sum_{i=1}^{N_T} e^{\iota 2\pi\beta d_T(i-1)s_i(t-\tau)}} \tag{5}$$

As per Equation (5), we can see that the measurements are just complex weighted combinations of the time-shifted version of the emitted signals. Hence, let the target be considered to be located on a delay-azimuth grid. For the sake of simplicity, we assume there are no off-grid errors which in general require additional post-processing steps.

The discrete version of the transmitted signal $\boldsymbol{s_i} \in C^{N_t}$ over the interval $[0, T)$ can be represented as follows:

$$\boldsymbol{s_i^T} = (s_i(0), s_i(\delta_t), \ldots, s_i((N_t-1)\delta_t))^T, \tag{6}$$

$$T = N_t\delta_t, \delta_t = 1/2B_c$$

We consider the sequences $\boldsymbol{s_i}$ transmitted to be period and band-limited to $(-B,B)$, where $B = LB_c$, hence as per Nyquist sampling theorem the signal $\boldsymbol{s_i}$ can be described completely in a discrete manner. We consider the target parameters β and τ to lie on an equidistant grid. We assume $\delta_\tau = 1/2B_c$ and $\delta_\beta = 2/N_TN_R$ as the discrete step sizes of the delay grid and azimuth grids, respectively.

As the received signals are just complex weighted combinations of the time-shifted version of the emitted signals, its discretised version is given by the following equation:

$$\boldsymbol{y_j^T} = \left(y_j(0), y_j(\delta_t), \ldots, y_j((N_t-1)\delta_t)\right)^T \in C^{N_t} \tag{7}$$

The received signal at the jth receiver depending on the target parameters can thus be approximated as follows:

$$\boldsymbol{y_j} = e^{\iota 2\pi c\lambda^{-1}\tau\delta_\tau} e^{\iota 2\pi \boldsymbol{d_R}\beta\delta_\beta(j-1)} \sum_{i=1}^{N_T} e^{\iota 2\pi \boldsymbol{d_T}\beta\delta_\beta(i-1)} \boldsymbol{T}_{\tau \boldsymbol{s_i}} \in C^{N_t} \tag{8}$$

where, $\boldsymbol{T_\tau}$ is a circulant shift matrix representing all shifted versions of the transmitted signal, such that $[\boldsymbol{T}_{\tau}\boldsymbol{s}]_k = [\boldsymbol{s}]_{k-\tau}$, and k-τ stands for subtraction modulo N_t. Hence, as a result of the periodicity operator $\boldsymbol{T}$ and the periodic influence of β as in Equation (8), the maximum possible grid points that can be achieved is bounded by $N_TN_RN_t$.

Next, we consider the generic model for the presence of multiple targets, which is given by the following equation:

$$\boldsymbol{y_j} = \sum_{k=1}^{K} \rho_k e^{\iota 2\pi c\lambda^{-1}\tau_k\delta_\tau} \tag{9}$$

$$\left[e^{\iota 2\pi \boldsymbol{d_R}\beta_k\delta_\beta(j-1)} \sum_{i=1}^{N_T} e^{\iota 2\pi \boldsymbol{d_T}\beta_k\delta_\beta(i-1)} \boldsymbol{T}_{\tau_k \boldsymbol{s_i}}\right] \in C^{N_t}$$

where $k = 1,\ldots,K \forall N$, is the number of targets and ρ_k its corresponding reflectivity.

Let $\boldsymbol{a_\gamma^j} \in C^{N_t}$ be a vector of target parameters corresponding to every jth receiver, such that,

$$\boldsymbol{a_\gamma^j} = e^{\iota 2\pi \boldsymbol{d_R}\beta\delta_\beta(j-1)} \sum_{i=1}^{N_T} e^{\iota 2\pi \boldsymbol{d_T}\beta\delta_\beta(i-1)} \boldsymbol{T}_{\tau \boldsymbol{s_i}}$$

$$\forall\, \gamma \in (\tau, \beta) \tag{10}$$

This allows the possibility of rewriting (9) efficiently as follows:

$$\boldsymbol{y_j} = \sum_{k=1}^{K} \rho_k e^{\iota k_0\tau_k\delta_\tau} \boldsymbol{a}^{\boldsymbol{j}}_{\gamma_k} \tag{11}$$

Therefore, any target scene imaged by this system can be considered a vector $\boldsymbol{x} \in C^N$, where $N = N_TN_RN_t$, being supported by indices of γ_k, which correspond to parameters of the target. Each non-zero entry of this vector $\boldsymbol{x}$ is occupied by a reflectivity, corresponding to the parameters of the targets, given by the following equation:

$$\boldsymbol{x}_{\gamma_k} = \rho_k e^{\iota k_0 c\tau_k\delta_\tau} \tag{12}$$

Finally, by collecting all signals from N_R receivers, we form a vector $\boldsymbol{y} \in C^M$, where $M = N_RN_t$. Then, we define a discrete grid target parameter space for the considered MIMO configuration. The grid space takes into consideration all possible delay samples and angular hypotheses with respect to each receiver element. By stacking each delay sample in combination with each azimuth as in Equation (10), we form a matrix $\boldsymbol{A} \in C^{M\times N}$.

$$\boldsymbol{A}_\gamma = \left(\left(\boldsymbol{a}_\gamma^{\boldsymbol{1}}\right)^T, \left(\boldsymbol{a}_\gamma^{\boldsymbol{2}}\right)^T, \ldots, \left(\boldsymbol{a}_\gamma^{\boldsymbol{N_R}}\right)^T\right)^T \in C^{M\times N} \tag{13}$$

Therefore, the linear relationship between the measurements collected from the MIMO system for a given target scene response $\boldsymbol{x}$ can be efficiently represented as follows:

$$\boldsymbol{y} = \boldsymbol{A}\boldsymbol{x} + \boldsymbol{n} \in C^{N_R N_t} \tag{14}$$

where, $\boldsymbol{y} \in C^{M\times 1}$ is a vector of measurements, $\boldsymbol{x} \in C^{N\times 1}$ is a sparse vector with target coefficients, $\boldsymbol{n} \in C^{N\times 1}$ is a vector of additive noise and $\boldsymbol{A} \in C^{M\times N}$ is the **sensing matrix**. We, thus have a highly underdetermined system (14), (as $M \ll N$) from which the target parameters (lying on the support set of $\boldsymbol{x}$) have to be reconstructed. This can be made possible via the use of CS algorithms.

2.1 | Compressed sensing theory

CS is a novel sampling theory that involves solving underdetermined systems of linear equations where the number of unknowns exceeds the available measurements [32]. In the context of parameter estimation using analogue sensors, CS facilitates the recovery of an unknown reflectivity vector $\boldsymbol{x} \in C^N$ from noisy measurements $\boldsymbol{y} \in C^M$. The relationship between $\boldsymbol{x}$ and $\boldsymbol{y}$ is approximated as $\boldsymbol{y} = \Theta\boldsymbol{x} + \boldsymbol{n}$, where $\boldsymbol{n} \in C^M$ represents measurement noise. In situations characterised as underdetermined (i.e. when $M \ll N$), it becomes evident that multiple solutions can satisfy the equation $\boldsymbol{y} = \Theta\boldsymbol{x}$. Consequently, the application of regularisation techniques becomes necessary to obtain a unique solution. An intriguing scenario arises when $\boldsymbol{x}$ exhibits sparsity, indicating that the number of non-zero elements is significantly smaller than the total elements in $\boldsymbol{x}$. In such cases, CS theory suggests that the sparse reflection vector can be accurately reconstructed using methods grounded in Convex Optimisation Algorithms such as Basis Pursuit, Greedy Pursuit Algorithms such as Orthogonal Matching Pursuit or Gradient Descent-Based Methods such as the Iterative Shrinkage-Thresholding Algorithm [19, 32].

Within the framework of Convex Optimisation-based approaches, the problem is formulated as given by the following equation:

$$\underset{\boldsymbol{x}}{\text{minimize}} \quad \|\boldsymbol{x}\|_{l_1} \quad \textit{subject to} \quad \|\Theta\boldsymbol{x} - \boldsymbol{y}\|_{l_2} \le \eta$$

In addition to the sparsity constraint, a critical factor contributing to the reliable recovery from an incomplete set of measurements is the inherent properties of the sensing matrix Θ.

One of the best-known metrics to measure sparse recovery properties of a sensing matrix (Θ) is the Restricted Isometry Property (RIP). The RIP uses the property of restricted isometric constant in order to establish the tightest performance guarantees currently known. For a given sparsity level S, the Restricted Isometry Constant (RIC) δ_S is the smallest positive constant such that,

$$(1-\delta_S)\|\boldsymbol{x}\|_{l_2}^2 \le \|\Theta\boldsymbol{x}\|_{l_2}^2 \le (1+\delta_S)\|\boldsymbol{x}\|_{l_2}^2 \tag{15}$$

holds for all vectors with $|\boldsymbol{x}|_0$ S, that is, the RIC establishes bounds for the singular values of the sub-matrices obtained by selecting any S columns from the complete Θ.

While the RIP is a reliable metric, there are major complications to consider when applying it.

1. Implementation challenges: In practical applications, it can be difficult to design measurement systems that meet the RIP conditions, especially for high-dimensional signals. Moreover, the RIP requires prior knowledge of the sparsity level of the signal, which may not be available in all cases.
2. Sensitivity to noise: The RIP assumes that measurements are noise-free, but in reality, noise is typically present. This can lead to violations of the RIP conditions, causing inaccuracies in signal recovery.
3. Computational complexity: Computing the RIP can be computationally intensive, particularly for large-scale problems. This can be a significant obstacle for real-time applications or those with limited computing resources.
4. Dependence on signal model: The RIP assumes that the signal is sparse or compressible in a specific basis. However, this assumption may not hold true for real-world signals, limiting the applicability of the RIP.

An alternative metric to the RIP is the MC μ of the sensing matrix $\boldsymbol{\Theta}$, which is defined as follows:

$$\mu(\Theta) = \max_{1\le i\ne j\le N} \frac{\left|\boldsymbol{\psi}_i^H \boldsymbol{\psi}_j\right|}{\|\boldsymbol{\psi}_i\|_2 \left\|\boldsymbol{\psi}_j\right\|_2} \tag{16}$$

where ψ_i is the *ith* column of $\boldsymbol{\Theta}$. MC has various advantages which make it desirable:

1. Matrix properties characterisation: The MC of a matrix is a useful quantitative measure of the correlation between its columns. This measure can help assess the suitability of a matrix for signal recovery algorithms that rely on sparsity or compressibility.
2. Algorithm performance analysis: The MC can be used to analyse the performance of signal recovery algorithms. For instance, the MC of the measurement matrix can be used to derive performance bounds for l_1-minimisation-based recovery algorithms [33].
3. Computational efficiency: The MC can be computed efficiently for any matrix without the need for complex algorithms, making it suitable for large-scale or multi-dimensional problems commonly encountered in real-time applications.

A lower MC value is associated with better CS performance, as it allows for more accurate signal recovery using fewer measurements. Therefore, in CS applications, designing sensing matrices with low MC is a common practice to improve the effectiveness of sparse signal recovery algorithms [32].

2.2 | Problem formulation

In the context of the model presented in Equation (14) and various radar applications, it is reasonable to assume that the distribution of targets within the angle-range domain exhibits sparsity. Consequently, techniques from CS algorithms can be employed to reconstruct the parameters of these targets, as discussed in ref. [34]. When exploring the use of sensing matrices in radar applications, the signal model of the sensing matrix is inherently influenced by the principles of signal propagation and the physical characteristics of the sensor [19]. As demonstrated in equation (10), it becomes evident that MC is a function of waveform characteristics, denoted as $\mu(\boldsymbol{A}(\boldsymbol{s}))$ as discussed in ref. [25]. In the specific context of a CDMA MIMO system, it is notably influenced by the inherent correlation properties found in the coded sequence. Therefore, the MC property within sensing matrices significantly influences the presence of sidelobes in radar systems. The imperative goal of minimising MC arises as a fundamental design objective with the aim of reducing sidelobes, thereby enhancing the accuracy and reliability of radar systems in the critical task of detecting and precisely locating targets or objects of interest. Thus, this study's primary objective is to design a novel coded sequence by minimising $\mu(\boldsymbol{A}(\boldsymbol{s}))$ adapted from the system defined in Equation (14).

3 | OPTIMISATION METHODOLOGY

In this section, we comprehensively describe the optimisation process in three key parts: (a) formulation, (b) approach and (c) assessment of convergence.

3.1 | a) Metric and constraints

In a MIMO system, the transmit sequences are required to exhibit both auto and cross-correlation responses. In the presence of a target, it is expected that the autocorrelation response for each transmit sequence maximises the AF and minimises the cross-ambiguity function responses. However, since there are no perfect orthogonal sequences, it often occurs that a mismatch between sequences, and sometimes within the sequences themselves, maximises the AF response, leading to extremely large sidelobes that cause masking and false alarms.

In general, an effective method to reduce the main lobe to sidelobe level (SLL) may involve considering sequences of larger lengths, as mentioned in ref. [35]. However, this approach increases the computational load of the MIMO system, and finding optimal polynomials that result in a unique combination of these long sequences is a finite set. If this condition is not satisfied, it may lead to problems arising from interference. An alternative approach would be to impose constraints on the maximum acceptable SLL for sequences of predetermined length. Additionally, within the CS framework, we can consider a randomly undersampled representation of the Match filter response for the simultaneously transmitted CDMA configuration as an effective equivalent to a complete set. Concisely as stated in ref. [36], based on the relationship between the AF response and sensing matrix coherence, we can assert that the MC of the sensing matrix corresponds to the second-highest peak resulting from the simultaneous cross-ambiguity response of all the sequences. Therefore, the MC of the sensing matrix for a MIMO system is related to the waveform correlation properties [25], including the highest cross-correlation between different lags of the same sequence and different lags between different sequences.

The objective of our study is to find the optimum combination of phase components for each transmit sequence with a constrained length and a maximum tolerable SLL so that the resultant sensing matrix has the lowest possible MC. To facilitate the solution, we incorporate the Gram matrix. The Gram matrix can be calculated as $\boldsymbol{G} = \hat{\boldsymbol{A}}(\boldsymbol{s})^H \hat{\boldsymbol{A}}(\boldsymbol{s})$, where $\hat{\boldsymbol{A}}(\boldsymbol{s})$ represents the sensing matrix with normalised columns. $\boldsymbol{G}$ efficiently represents the Match filter response and subsequently the joint ambiguity and cross-ambiguity response, with *of* $\mu\left(\hat{\boldsymbol{A}}(\boldsymbol{s})\right)$ defining the highest sidelobe. Specifically, the Gram matrix indicates the interference caused by each sequence to itself and to others. Its block diagonal elements show the power of each sequence and, subsequently, their main lobe widths, while the off-diagonal elements indicate interference within and between sequences. It is important to note that using perfectly orthogonal waveforms results in a diagonal Gram matrix, where all off-diagonal elements are zero. This diagonal Gram matrix ensures that the waveforms are orthogonal, minimising interference and maximising the system's Signal-to-Interference-plus-Noise Ratio (SINR). Finally, it's important to note that the Gram matrix is Hermitian and can be visualised as follows:

$$\mathbf{G} = \begin{bmatrix} g_{1,1} & g_{1,2} & \cdots & g_{1,N-1} & g_{1,N} \\ g_{1,2}^* & g_{2,2} & & g_{2,N-1} & g_{2,N} \\ \vdots & & \ddots & \vdots & \\ g_{1,N-1}^* & g_{2,N-1}^* & \cdots & g_{N-1,N-1} & g_{N-1,N} \\ g_{1,N}^* & g_{2,N}^* & & g_{N-1,N}^* & g_{N,N}^* \end{bmatrix}$$

The objective is to design a sensing matrix with the lowest possible MC, indicating a Gram matrix with minimal magnitudes in its off-diagonal elements. Therefore, we exclude the principal diagonal elements (p.d.e.) by considering $\hat{\boldsymbol{G}} = |\boldsymbol{G} - \boldsymbol{I}|$. Since $\hat{\boldsymbol{G}}$ is Hermitian, the resulting MC values can be represented using only the upper triangular elements. Additionally, since the secondary diagonals around the p.d.e, represent the width main lobe, we introduce a calibre term to avoid penalising the main lobes. This ensures focus on the sidelobes. The calibre is calculated as a half power beam width as adapted from ref. [37], and can be taken as the number of c secondary diagonals to be excluded. The resulting elements are stacked in as a vector $\boldsymbol{g} \in C^{N_c(N_c-1)/2}$, with N_c the off-diagonal

excluding the main lobe width. The maximum SLL is, thus, represented as the infinity norm of the set, given by $\|\mathbf{g}\|_\infty$.

Since our study concentrates on sequences of predetermined length with a maximum accepted SLL, we impose an additional constraint on the maximum acceptable SLL, denoted as TolSLL. The tolerance is calculated as a value lower than metric described in tab. 3.2 of ref. [38]. The optimisation problem is, thus, formulated as follows:

$$\min_{\boldsymbol{\phi}} \|\mathbf{g}\|_\infty$$

$$s.t. \quad g = \mathrm{i}\neq\mathrm{j}\frac{\left|\boldsymbol{a}_i^H \boldsymbol{a}_j\right|}{\|\boldsymbol{a}_i\| \, \|\boldsymbol{a}_j\|} \tag{17}$$

$$-\pi \leq \boldsymbol{\phi} \leq \pi$$

$$\|\mathbf{g}\|_\infty < \mathrm{Tol}_{\mathrm{SLL}}$$

3.2 | b) Approach

Equation (17) presents an optimisation problem with the objective of minimising MC or the highest SLL within each delay-azimuth bin, as characterised by the sensing matrix in Equation (14). The total number of phase components transmitted simultaneously by N_T transmit elements serves as the optimisation parameters. The objective is to identify the optimal combination of phase components, subject to constraints within a defined search space and under the limitation of the highest acceptable value.

To begin, this problem belongs to the category of combinatorial search problems, which involve identifying the best solution or arrangement from a finite set. Generally, this set can be extensive, leading to computational challenges as the problem size increases. Additionally, the relationship between the parameters and the cost function is non-linear, necessitating the use of solvers capable of handling non-linearities.

Furthermore, the cost function of interest focuses on the highest SLL, which is characterised by the Gram matrix. This matrix's second-largest eigenvalue serves as a measure of the coherence of the sensing matrix, as discussed in ref. [39] section 8.3.1. Formulations of a Gram matrix can be treated as a convex problem provided that the underlying Gram matrix is positive semidefinite. This requirement, in turn, mandates that the underlying sensing matrix has unique columns, resulting in all eigenvalues being greater than zero.

The primary objective of this optimisation problem is to design a sensing matrix with unique columns, a property lacking in the initialised configuration. Hence, we can assert that the optimisation problem in Equation (17) is non-convex and, as recommended in the literature [40], necessitates the utilisation of global optimisers. In our case, Simulated Annealing (SA) [41] has been chosen as the algorithm to minimise $\mu\left(\hat{\boldsymbol{A}}(\boldsymbol{s})\right)$ by optimising $\boldsymbol{\phi}$, as described in Algorithm 1.

Algorithm 1 Sequence optimisation via mutual coherence minimisation of delay-azimuth sensing matrix

Data: FTCDMA MIMO radar sensing matrix $\mathbf{A}$, phase components of sequences ϕ
Result: Optimized FTCDMA MIMO sensing matrix $\mathbf{A}$, optimum orthogonal sequence $\tilde{\phi}$
Input : Number of rows M, number of columns N, sequence length $N_T L$, initial sequence phase ϕ_0, initial temperature T_0, cooling rate α, maximum number of iterations Max_iter
Output: Optimized FTCDMA MIMO sensing matrix $\mathbf{A}$,optimum orthogonal sequence $\tilde{\phi}$

Initialize the FTCDMA MIMO sensing matrix $\mathbf{A}$ with initial Hadamard sequence; Set the initial temperature $T = T_0$;
for $i = 1$ *to* Max_{iter} **do**
  Generate a new candidate solution by randomly perturbing the phase components of the support sequences in the FTCDMA MIMO sensing matrix $\mathbf{A}(\mathrm{s})'$; Evaluate the new candidate solution by computing the mutual coherence $\mu(\mathbf{A}(\mathrm{s})')$ of the perturbed FTCDMA MIMO sensing matrix $\mathbf{A}(\mathrm{s})'$;
  if $\mu(\mathbf{A}(\mathrm{s})') < \mu(\mathbf{A}(\mathrm{s}))$ **then**
    Accept the new candidate solution as the current solution $\mathbf{A}(\mathrm{s})$, store new ϕ';
  else
    Accept the new candidate solution with probability $p = \exp\left(-\frac{\mu(\mathbf{A}(\mathrm{s})') - \mu(\mathbf{A}(\mathrm{s}))}{T}\right)$;
    if *Accepted* **then**
      Set the new candidate solution as the current solution $\mathbf{A}(\mathrm{s})$;
  Reduce the temperature $T = \alpha T$;
Output the final FTCDMA MIMO sensing matrix $\mathbf{A}(\mathrm{s})$ and new optimised ϕ;

3.3 | c) Assessment of convergence

Simulated Annealing is a stochastic optimisation approach inspired by the annealing processes employed in metallurgy. It excels in finding nearly optimal solutions within complex search spaces, particularly in situations where identifying the best solution through exhaustive search becomes a challenging endeavour. The algorithm operates with a temperature schedule that dictates the cooling rate. Initially, it extensively explores the search space at high temperatures and gradually reduces the temperature to concentrate on exploiting the best-known solutions. A common variant of the algorithm involves stopping after a specified maximum number of iterations or when a temperature threshold is reached.

In general, SA can lead to multiple local minima in the cost function. In this specific context, this can result in phase configurations with low MC values but the potential for high sidelobes within different sequence combinations. Therefore, we have adapted the generic SA algorithm to accommodate constraints on the maximum tolerable SLL over multiple iterations.

As an engineering refinement, the conventional SA algorithm has undergone two key modifications. Firstly, subtle random jumps have been introduced into the search variations to prevent convergence at local minima, thereby enabling the discarding of sub-optimal solutions. Secondly, a flood buffer has been incorporated to facilitate the algorithm's persistence in searching for a recurring configuration that minimises the cost function. These adjustments are depicted in Figure 1, where configurations with low MC values trigger the exploration of multiple similar configurations, as denoted by the blue circles. The recurrence of a configuration is determined by evaluating $\left|\boldsymbol{s}^{iter+1} - \boldsymbol{s}^{iter}\right| < e$, (where e is an error threshold) and updating the flood buffer accordingly. The buffer floods when 10% of total elapsed iterations yield the same or nearly identical sequence vectors, as indicated by the clustering of multiple blue circles around a specific area near the intersection of the preferred SLL and obtained MC value. This process ensures the identification of a relatively optimal configuration from among multiple sub-optimal solutions. Figure 2 illustrates the reduction in MC minimisation, with MC values stabilising towards the end of the process and termination occurring upon reaching the recurring configuration over multiple iterations. The optimisation problem yields a sensing matrix with low MC, reflected in the new poly-phase sequences characterised by high autocorrelation and low cross-correlation. These sequences are highly suitable for implementation in CDMA MIMO radar systems. Despite potential suboptimality, the obtained sequence remains optimal for reconstruction using CS algorithms.

To assess the proposed sequence, we conducted a comparative study against sequences commonly used in MIMO literatures [38, 42–44]. This study involved using Doppler cuts of the ambiguity and cross-ambiguity function responses and graphically presenting the variation of Peak Sidelobe Level (PSLL) and Integrated Sidelobe Level (ISLL) for different code lengths as shown in Figure 3. Additionally, we compared the results obtained from recent publications [35, 38, 45–48], which also focus on similar design strategies for generating poly-phase sequences. In these comparisons, we utilised the PSLL and ISLL information tabulated in these studies as reference values against the values obtained from our optimised sequence. Since the values in the literature encompass varying configurations between lengths of 64 and 128, we set the proposed sequence to a length of 100 for comparison purposes. Table 1 presents a comparison of the autocorrelation responses, while Table 2 compares the cross-correlation responses.

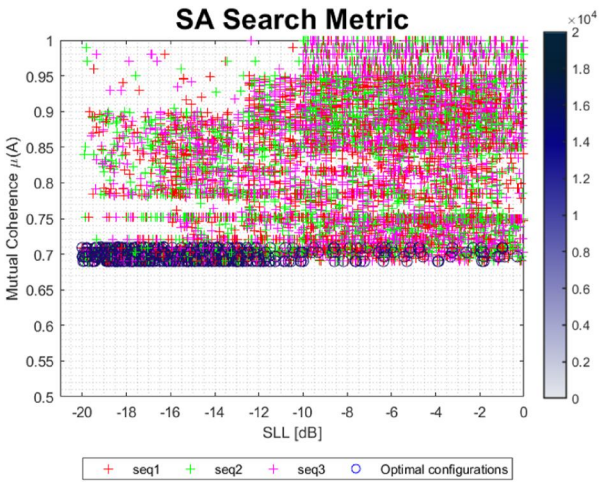

FIGURE 1 Illustrates the progression of the search for the optimal phase sequence combinations during the SA algorithm iterations. Different-coloured '+' markers represent various combinations of each input sequence, while 'o' markers denote the optimal combinations, considering calibre and SLL threshold. The colour bar indicates the number of iterations. Repeated circles mark the convergence to a preferred optimum solution and prompting the termination of search.

4 | SIMULATION RESULTS

We consider a Uniform Linear Array configuration, with 3 transmitters and 4 receivers. We assume antenna arrays to be omnidirectional, operating under ideal conditions. We consider 3 different families of sequences: Hadamard, Gold and an arbitrarily chosen poly-phase sequence to be transmitted from the 3 emitters. We compare the three candidates against the optimised sequence using the CS algorithm BPDN [33].

The optimised sequence has been evaluated based on two aspects:

4.1 | Quality of the sensing matrix

The quality of a sensing matrix, often referred to as 'measurement quality' or 'sensing system quality', relates to how effectively the parameters within the sensing matrix have been engineered. It ensures the collected information or measurements from a target, represented by the rows of **y**, can be

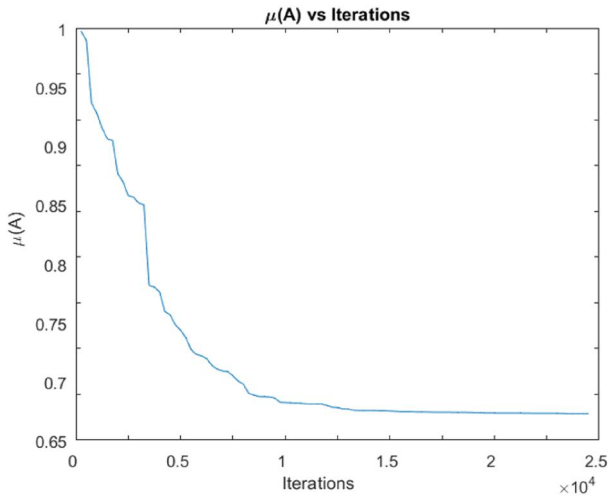

FIGURE 2 Displays the mutual coherence minimisation over global optimiser iterations. The graph shows a stable value over multiple iterations, signifying a full buffer and the initiation of the stopping condition.

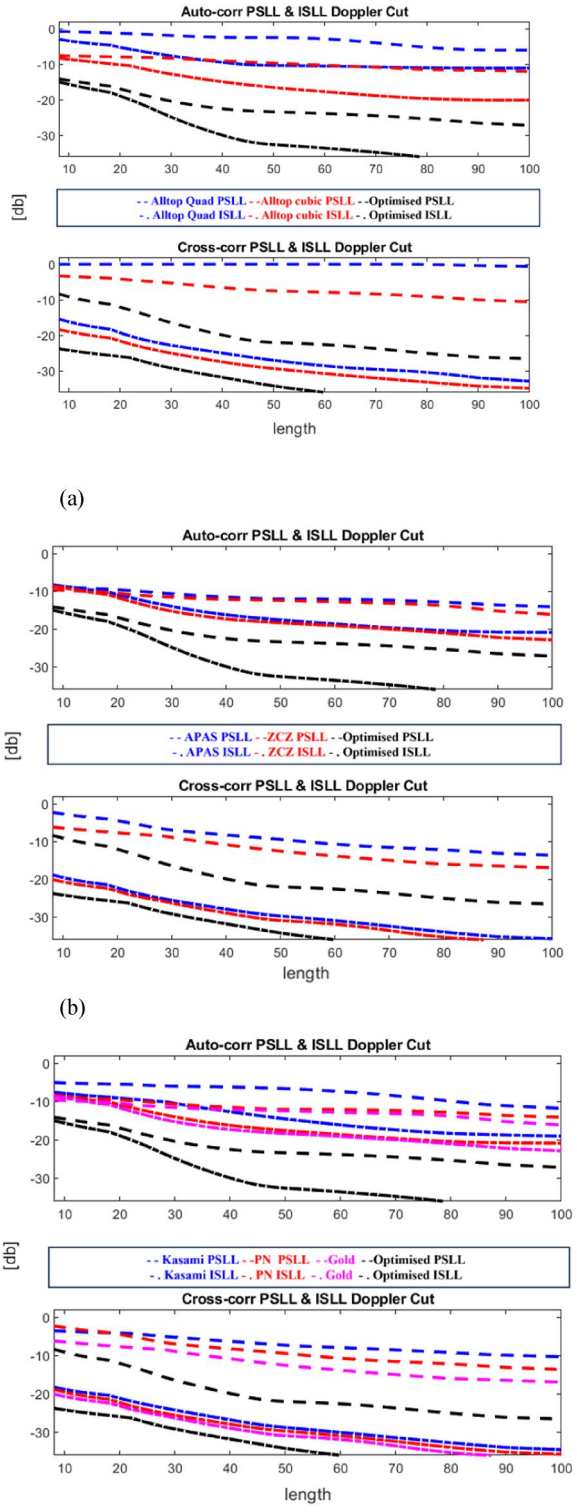

FIGURE 3 Presents a comparative analysis of the Peak-to-Sidelobe Level (PSLL) and Integrated Sidelobe Level (ISLL) for the proposed sequence at various lengths, contrasted with different candidate sequences. Sub-figures (a) compare it against Alltop quad and cube sequences, (b) against APAS and ZCZ sequences, and (c) against Kasami, Gold, and PN sequences.

TABLE 1 Autocorrelation response comparison.

Sequence	PSLL (dB)	ISLL (dB)	Length
Proposed	−27.76	42	100
MA-AMISL [45]	−26.55	72.33	64
[46]	−28	-	256
[47]	−23	100	256
[48] CAN, WeCAN, CA	−20.54, −31.10, −21.08	-	256
[35]	−29	40	128
[38]	−21.87	-	100

TABLE 2 Cross correlation response comparison.

Sequence	PSLL (dB)	ISLL (dB)	Length
Proposed	−26.24	43	100
MA-AMISL [45]	−16.55	72.33	64
[46]	−30	-	256
[47]	−19	100	256
[48] CAN, WeCAN, CA	−18.19, −29.89, −20.77	-	256
[35]	−17	40	128
[38]	−19.24	-	100

clearly associated with the columns of **A** and, subsequently, with the rows of **x**. This assessment relies on a range of metrics, encompassing structural characteristics such as incoherency and spectral metrics such as the response of the AF, along with eigenvalues characterised by Gerschgorin discs.

4.2 | Sparse reconstruction performance

Sparse reconstruction performance refers to the ability of an algorithm or method to accurately reconstruct a sparse signal or data from a limited set of measurements or observations, under different realisations of the observed scene.

An optimally designed family of sequences would ensure a highly incoherent sensing matrix, resulting in a Gram matrix with lesser smearing around principle diagonal elements, meaning lower correlation between the columns. This directly would translate to lower sidelobe levels, improved AF response, higher recovery percentages and lower recovery errors.

4.2.1 | Quality metrics

- **Incoherency:**

A sensing matrix is considered incoherent when its columns exhibit maximal dissimilarity, leading to enhanced precision and

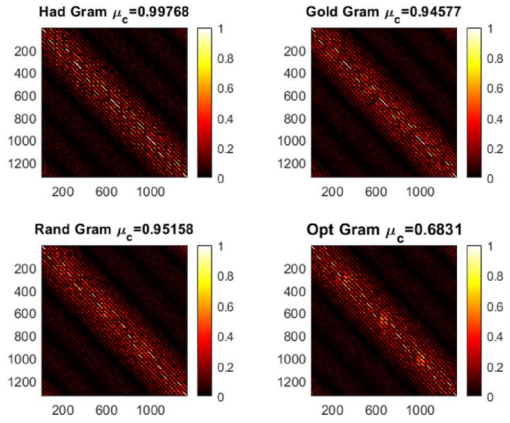

FIGURE 4 Comparing Gramian matrices for different candidate sequences, clockwise from top left: Hadamard, Gold, arbitrary poly-phase, and optimised Sequences.

efficiency in signal recovery. We gauge this incoherence by quantifying the MC between the columns of the sensing matrix using the Gram matrix. MC corresponds to the highest off-diagonal elements in the Gram matrix, resulting in low MC when the off-diagonal elements of the corresponding Gram matrix approach their theoretical lower bound [49], and the diagonal elements are equal to one. This characteristic is pivotal in Compressive Sensing (CS) because a Gram matrix approaching an identity matrix bears witness to a certain isometric behaviour of the sensing matrix. In other words, the underlying sensing matrix preserves the geometry of the problem in its original space. In Figure 4, we present a visual comparison of the various Gram matrices associated with each sensing matrix under consideration.

- **AF:**

The AF response is a measure of the interference caused by the range and Doppler of a target in comparison to a reference target of equivalent RCS. It can be represented by a function that takes two input variables, range and Doppler, and outputs a value representing the level of interference. The Gram matrix can be used to calculate the AF response for a set of waveforms by taking the inner product of the waveforms. The AF response can be expressed as a sum of the products of the waveforms and their complex conjugates, with each term weighted by the corresponding element in the Gram matrix. In Equation (17), the cost function is aimed at minimising the maximum off-diagonal elements of the Gram matrix by tuning the transmitted sequences; this is an indirect way of optimising the AF of the waveforms, and as it is shown in Figure 5.

We can see that the optimised sequence has lower sidelobes and improved resolution compared to the initial Hadamard sequence.

- **Gerschgorin discs:**

The Gershgorin Disc Theorem is employed to establish bounds on the eigenvalues of complex square matrices. Similarly, the RIP relies on the eigenvalues of the Gram matrix, which results from the inner product of the columns of the sensing matrix. The RIP ensures that the sensing matrix preserves the sparsity of the signal, facilitating precise signal recovery. Crucially, the eigenvalues of the Gram matrix play a pivotal role in our understanding of MC. When the off-diagonal entries of the Gram matrix approach their theoretical lower bound [49], it signifies low MC. Hence, it's evident that a relationship exists between the Gershgorin theorem and the MC of the sensing matrix. The Gershgorin Disc can also be employed to establish bounds for MC.

In the complex plane, each Gershgorin disc, denoted as D_i and centred at $a_{i,i}$ with a radius $R_i = \sum |a_{i,j}|$ [50], is defined as follows:

$$D_i = \left\{ z \in C : |z - a_{i,i}| \leq \sum_{j=1, j\neq i}^{n} |a_{i,j}| \right\}, i = 1, \ldots, n \quad (18)$$

where C represents the set of complex numbers, and $a_{i,j}$ is the entry in the *ith* row and *jth* column of matrix $\hat{A}(s)$.

In situations involving MC, the eigenvalues of a sensing matrix with low MC tend to cluster around the largest eigenvalue. Additionally, the radius of the Gershgorin discs, as per Equation (18) is relatively smaller. This condition ensures better signal recovery compared to a Gram matrix with relatively high MC.

In Figure 6, we assess the Gerschgorin disks for various candidate sequences by computing the sum of K randomly selected off-diagonal elements from the Gramian matrices corresponding to each row. The table in Table 3, presents the percentage reduction in the Gerschgorin disk radii compared to the Hadamard sequence.

4.2.2 | Reconstruction performance metrics

- **Recovery Percentage:**

The recovery percentage represents the ratio of accurately estimated targets to the total number of targets within a specific scene. The improvement in recovery can be attributed to the quality of the sensing matrix, which is determined by its MC. A lower MC is associated with better recovery percentage. To ensure the accuracy of this metric, we conducted Monte Carlo simulations, varying the number of targets and their placement across different delay-azimuth bins. In Figure 7, you can observe the recovery percentages across a range of sparsity orders, from 1 to 50. The results clearly demonstrate that the optimised sequences outperformed all other tested candidates, mainly due to their reduced MC, which directly contributed to enhanced reconstruction efficiency.

- **Recovery error:**

The recovery error within a target scene refers to the disparity between the estimated target position and its actual

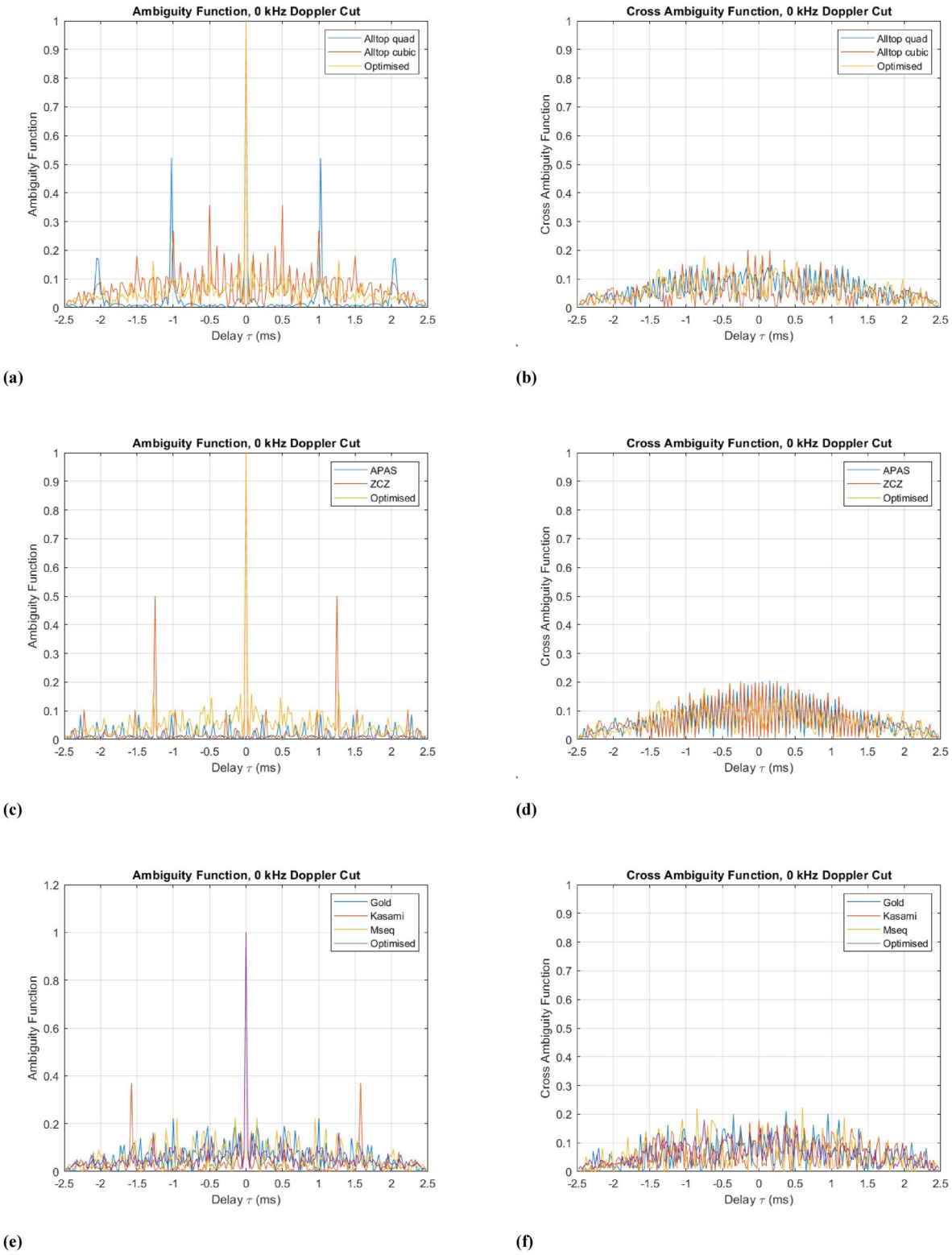

FIGURE 5 Illustrates a comparative analysis of correlation responses between the proposed optimised sequence and conventionally used sequences for CDMA MIMO transmission. Sub-figures (a), (c), and (e) depict the autocorrelation responses with delay-cut for ambiguity reduction, while sub-figures (b), (d), and (f) represent the cross-correlation responses with delay-cut in the cross-ambiguity function response. The results clearly demonstrate the superior performance of the optimised sequence compared to existing state-of-the-art solutions.

position on a discrete grid scene, which is quantified as $\|\hat{\boldsymbol{x}} - \boldsymbol{x}\|$. The precision of the recovery is a direct outcome of designing sensing matrices with nearly orthogonal columns, and this is quantified by the concept of MC. In essence, lower MC leads to lower recovery errors. This performance metric is assessed under two scenarios: first, when the number of targets

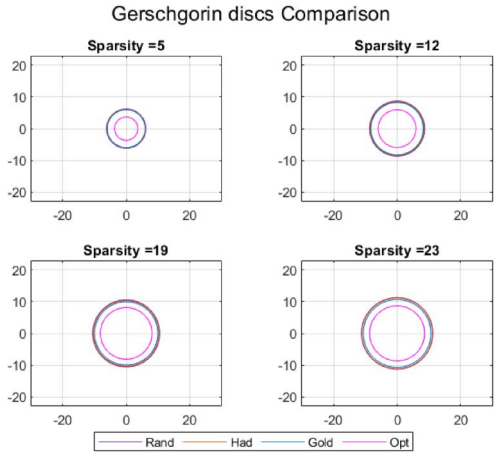

FIGURE 6 Comparison of the Gerschgorin discs of candidate sequences for Gram matrices restricted by different sparsities K. It can be seen that the optimal sequence has the smallest radius in comparison to all other candidates.

TABLE 3 % Radii reduction comparison.

	Arbitrary	Gold	Optimised
Sparsity 5	39.14	39.98	41.14
Sparsity 12	26.52	28.75	30.03
Sparsity 19	13.86	17.42	18.73
Sparsity 23	13.05	16.59	18.53

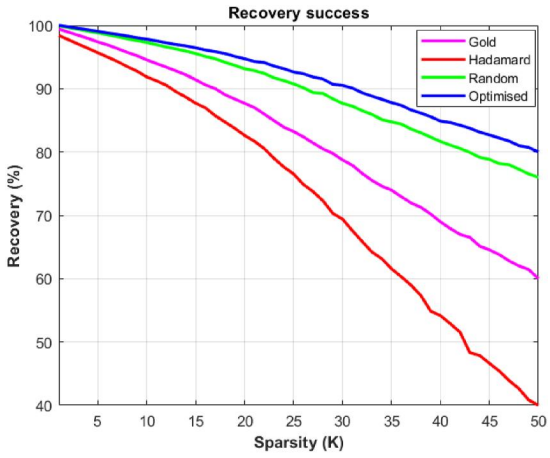

FIGURE 7 Recovery percentage versus sparsity (K), where different sparsity order $1 \leq K \leq 50$ over 1000 iteration.

remains constant while their signal strengths vary (across SNR values ranging from −20 to 20 dB, as illustrated in Figure 8); and second, when the sparsity order varies while maintaining a constant SNR value (as depicted in Figure 9). Each scenario is evaluated through Monte Carlo simulations conducted over 1000 runs. The results consistently show that the optimised sequence outperforms the other candidates in both cases.

To illustrate the stability of the sequence in the presence of noise, we compare the same sequence for 3 cases namely, (low SNR) −3 db, 0 db SNR and (high SNR) 3db. Monte Carlo

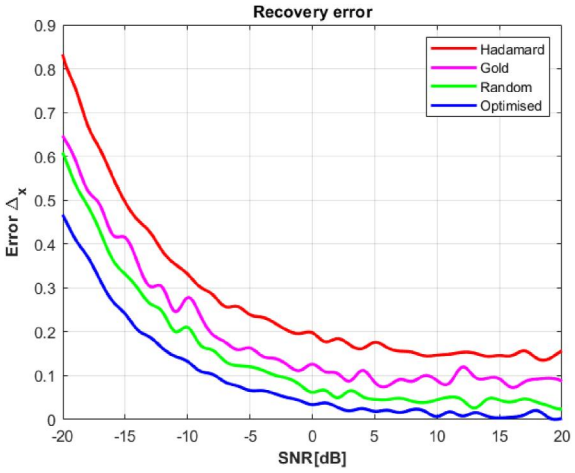

FIGURE 8 Comparison of estimation error for $K = 10$, at different SNR cases.

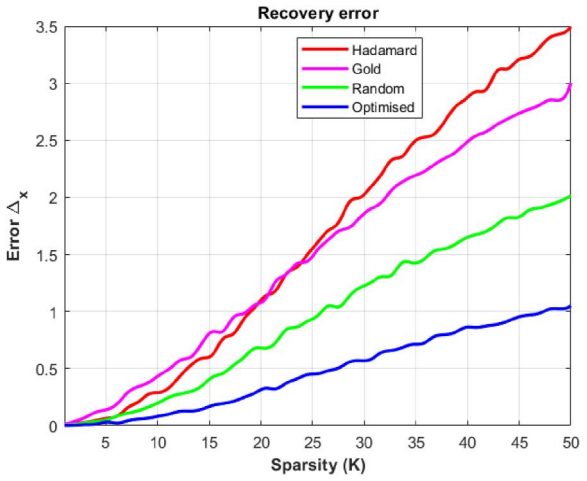

FIGURE 9 Comparison of estimation error for SNR = 0 dB, with different number of targets.

simulations are conducted for 1000 runs in each scenario. The results of the analysis are as in Figure 10.

5 | CONCLUSION

In conclusion, this research article addresses a crucial aspect of waveform design for Code Division Multiple Access Multiple Input Multiple Output (CDMA-MIMO) radar systems, with a specific focus on enhancing CS-based target estimation. The study introduces an optimisation framework for modifying phase components in CS-CDMA MIMO sequences, with the ultimate goal of minimising the infinity norm, of off-diagonal elements in the Gramian matrix of the sensing matrix. This research represents a significant contribution to the field, as it tackles a complex, non-convex and combinatorial optimisation problem using the SA algorithm. The comparative analysis against established sequences, such as Hadamard and Gold sequences showcases the superiority of the generated poly-

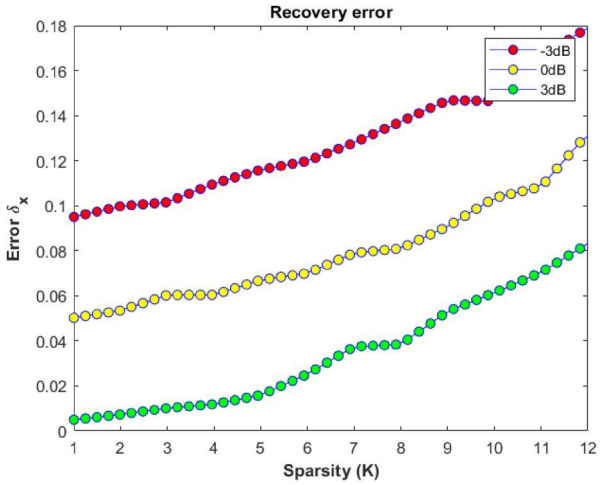

FIGURE 10 Optimised Sequence performance for different noise levels.

phase sequences. These sequences exhibit exceptional performance in terms of correlation properties, AF behaviour, recovery percentage and recovery error, thereby significantly improving target reconstruction results in CDMA-MIMO radar systems employing CS-based estimation. Furthermore, this study expands the horizon of waveform design by focusing on adjusting parameters within each pulse or during the fast-time interval, offering new avenues for research in the realm of CS-based CDMA MIMO radar.

5.1 | Future scope

The process of identifying tuneable parameters to optimise radar systems, which play a critical role as conduits to induce incoherence in an underlying sensing matrix, necessitates a comprehensive and computationally expensive optimisation approach [51]. However, once such parameter is identified and the mere application of this concept can be modelled as a projection matrix. Additionally, this projection matrix (if designed correctly) can serve as a means to exploit signal sparsity, in addition to the conventional scene sparsity imposed by basis transformation matrices [32]. A demonstration of this concept was published in our earlier study [52], where we designed a sparse random array based on MC minimisation. Building upon the concepts of our current and past studies, our future work will focus on defining MC as a design metric for sparsity-aware radar systems, which will be achieved through the careful design of a sparsifying randomised projection matrix.

5.2 | Application scope

Typically, a MIMO radar system that achieves transmit orthogonality through FT-CDMA can be applied in various scenarios, provided that the relatively high sidelobes in the range domain are deemed acceptable, as highlighted by H. Sun [3]. One particularly promising application for the findings of this study lies within automotive systems, especially in the context of fully automated driving vehicles, which are expected to become more prevalent [53]. Nevertheless, as we venture further into complete automation, concerns arise regarding the potential masking of weaker targets by the high sidelobes of stronger targets, which become a paramount issue. Our study indicates that these concerns can be effectively addressed by combining FT-CDMA with SSP. Additionally, through the design of incoherent sequences, we have introduced enhancements to the performance of the SSP-based system. Assuming the development of a system that can support FT-CDMA, we firmly believe that our research will be invaluable in realising fully automated driving scenarios in the near future.

AUTHOR CONTRIBUTIONS

Saravanan Nagesh: Conceptualisation; data curation; formal analysis; investigation; methodology; resources; software; validation; visualisation; writing – original draft. **María A. González-Huici:** Funding acquisition; supervision; validation. **Andreas Bathelt:** Project administration; writing – review & editing. **Miguel Heredia Conde:** Formal analysis; project administration; writing – review & editing. **Joachim Ender:** Conceptualisation; funding acquisition; supervision.

ACKNOWLEDGEMENTS

This project has received funding from the European Union's Horizon 2020 research and innovation program under Marie Sklodoska-Curie grant agreement No. 860370.

Open Access funding enabled and organized by Projekt DEAL.

CONFLICT OF INTEREST STATEMENT

The authors declare no conflicts of interest.

DATA AVAILABILITY STATEMENT

Research data are not shared.

ORCID

Saravanan Nagesh https://orcid.org/0000-0003-4266-0405

REFERENCES

1. Richards, M.A.: Fundamentals of Radar Signal Processing. McGraw-Hill Professional (2005)
2. Gini, F., De Maio, A., Lee, P. (eds.) Waveform Design and Diversity for Advanced Radar Systems. Institution of Engineering; Technology (2012). https://doi.org/10.1049/pbra022e
3. Sun, H., Brigui, F., Lesturgie, M.: Analysis and comparison of MIMO radar waveforms. In: 2014 International Radar Conference, Lille, France, pp. 1–6 (2014). https://doi.org/10.1109/RADAR.2014.7060251
4. Anitori, L., Ender, J.: Waveform design for sparse signal processing in radar. In: 2021 IEEE Radar Conference (RadarConf21), Atlanta, GA, USA, pp. 1–6 (2021). https://doi.org/10.1109/RadarConf2147009.2021.9455313
5. Uysal, F.: Phase-coded FMCW automotive radar: system design and interference mitigation. IEEE Trans. Veh. Technol. 69(1), 270–281 (2020). https://doi.org/10.1109/TVT.2019.2953305
6. Liu, G., Gu, H., Su, W.: Development of random signal radars. IEEE Trans. Aero. Electron. Syst. 35(3), 770–777 (1999). https://doi.org/10.1109/7.784050

7. Norland, R.: Digital signal processing in binary phase coded CW multistatic radar. In: 2003 Proceedings of the International Conference on Radar (IEEE Cat. No.03EX695), Adelaide, SA, Australia, pp. 299–302 (2003). https://doi.org/10.1109/RADAR.2003.1278756
8. Davis, R.M., Fante, R.L., Perry, R.P.: Phase-coded waveforms for radar. IEEE Trans. Aero. Electron. Syst. 43(1), 401–408 (2007). https://doi.org/10.1109/TAES.2007.357142
9. Benedetto, J.J., Konstantinidis, I., Rangaswamy, M.: Phase-coded waveforms and their design. IEEE Signal Process. Mag. 26(1), 22–31 (2009). https://doi.org/10.1109/MSP.2008.930416
10. Bourdoux, A., et al.: PMCW waveform and MIMO technique for a 79 GHz CMOS automotive radar. In: 2016 IEEE Radar Conference (RadarConf), Philadelphia, PA, USA, pp. 1–5 (2016). https://doi.org/10.1109/RADAR.2016.7485114
11. Haderer, H., Feger, R., Stelzer, A.: A comparison of phase-coded CW radar modulation schemes for integrated radar sensors. In: 44th European Microwave Conference, Rome, Italy, pp. 1896–1899 (2014). https://doi.org/10.1109/EuMC.2014.6986832
12. Matousek, Z., et al.: Doppler compensation for binary phase-coded radar signals in presence of noise jamming. In: 2016 17th International Radar Symposium (IRS), Krakow, Poland, pp. 1–4 (2016). https://doi.org/10.1109/IRS.2016.7497318
13. Overdevest, J., et al.: Doppler influence on waveform orthogonality in 79 GHz MIMO phase-coded automotive radar. IEEE Trans. Veh. Technol. 69(1), 16–25 (2020). https://doi.org/10.1109/TVT.2019.2951632
14. Kumbul, U., et al.: Phase-coded FMCW for coherent MIMO radar. IEEE Trans. Microw. Theor. Tech. 71(6), 2721–2733 (2023). https://doi.org/10.1109/TMTT.2022.3228950
15. He, H., Stoica, P., Li, J.: Designing unimodular sequence sets with good correlations—including an application to MIMO radar. IEEE Trans. Signal Process. 57(11), 4391–4405 (2009). https://doi.org/10.1109/TSP.2009.2025108
16. Raei, E., et al.: Range-ISL minimization and spectral shaping in MIMO radar systems via waveform design. In: ICASSP 2023 - 2023 IEEE International Conference on Acoustics, Speech and Signal Processing (ICASSP), Rhodes Island, Greece, pp. 1–5 (2023). https://doi.org/10.1109/ICASSP49357.2023.10096518
17. Baraniuk, R., Steeghs, P.: Compressive radar imaging. In: 2007 IEEE Radar Conference, Waltham, MA, USA, 128–133 (2007). https://doi.org/10.1109/RADAR.2007.374203
18. Herman, M.A., Strohmer, T.: High-resolution radar via compressed sensing. IEEE Trans. Signal Process. 57(6), 2275–2284 (2009). https://doi.org/10.1109/TSP.2009.2014277
19. Ender, J.H.G.: On compressive sensing applied to radar. Signal Process. 90(5), 1402–1414. (2010). https://doi.org/10.1016/j.sigpro.2009.11.009
20. ishra, K.V., Eldar, Y.C.: Sub-Nyquist Radar: Principles and Prototypes (2019). https://arxiv.org/abs/1803.01819
21. Mishra, K.V., et al.: A cognitive sub-nyquist MIMO radar prototype. IEEE Trans. Aero. Electron. Syst. 56(2), 937–955 (2020). https://doi.org/10.1109/TAES.2019.2924163
22. Liu, C., et al.: Pulse-Doppler signal processing with quadrature compressive sampling. IEEE Trans. Aero. Electron. Syst. 51(2), 1217–1230 (2015). https://doi.org/10.1109/TAES.2014.130475
23. Shastry, M.C., et al.: Analysis and design of algorithms for compressive sensing based noise radar systems. In: 2012 IEEE 7th Sensor Array and Multichannel Signal Processing Workshop (SAM), Hoboken, NJ, USA, pp. 333–336 (2012). https://doi.org/10.1109/SAM.2012.6250503
24. Shastry, M.C., Narayanan, R.M., Rangaswamy, M.: Waveform design for compressively sampled ultrawideband radar. J. Electron. Imag. 22(2), 021011 (2013). https://doi.org/10.1117/1.jei.22.2.021011
25. Entezari, R., Rashidi, A.: Incoherent waveform design for compressed sensing radar based on pulse-train scenario. IET Commun. 12(17), 2132–2136 (2018). https://doi.org/10.1049/iet-com.2018.5287
26. Hu, H., et al.: Locating the few: sparsity-aware waveform design for active radar. IEEE Trans. Signal Process. 65(3), 651–662 (2017). https://doi.org/10.1109/TSP.2016.2620966
27. Zhang, J., Zhu, D., Zhang, G.: Adaptive compressed sensing radar oriented toward cognitive detection in dynamic sparse target scene. IEEE Trans. Signal Process. 60(4), 1718–1729 (2012). https://doi.org/10.1109/TSP.2012.2183127
28. Ender, J.: A brief review of compressive sensing applied to radar. In: 2013 14th International Radar Symposium (IRS), vol. 1, pp. 3–16 (2013)
29. van Rossum, W., Anitori, L.: Doppler ambiguity resolution using random slow-time code division multiple access MIMO radar with sparse signal processing. In: 2018 IEEE Radar Conference (RadarConf18), Oklahoma City, OK, USA, pp. 0441–0446 (2018). https://doi.org/10.1109/RADAR.2018.8378599
30. Tohidi, E., et al.: Sparse antenna and pulse placement for colocated MIMO radar. IEEE Trans. Signal Process. 67(3), 579–593 (2019). https://doi.org/10.1109/tsp.2018.2881656
31. Nagesh, S., Ender, J., González–Huici, M.A.: Influence of waveform orthogonality and array geometry on compressed sensing algorithms for CDMA MIMO radar. In: 2022 14th German Microwave Conference (GeMiC), Ulm, Germany, pp. 76–79 (2022)
32. Donoho, D.L.: Compressed sensing. IEEE Trans. Inf. Theor. 52(4), 1289–1306 (2006). https://doi.org/10.1109/TIT.2006.871582
33. van den Berg, E., Friedlander, M.P.: Sparse Optimization with Least-Squares Constraints. Tech. Rep. TR-2010-02. Dept of Computer Science, Univ of British Columbia (2010)
34. Dorsch, D., Rauhut, H.: Refined Analysis of Sparse MIMO Radar (2015)
35. Esmaeili-Najafabadi, H., Ataei, M., Sabahi, M.F.: Designing sequence with minimum PSL using Chebyshev distance and its application for chaotic MIMO radar waveform design. IEEE Trans. Signal Process. 65(3), 690–704 (2017). https://doi.org/10.1109/TSP.2016.2621728
36. Song, X., Zhou, S., Willett, P.: The role of the ambiguity function in compressed sensing radar. In: 2010 IEEE International Conference on Acoustics, Speech and Signal Processing, Dallas, TX, USA, pp. 2758–2761 (2010). https://doi.org/10.1109/ICASSP.2010.5496221
37. Mateos-Núñez, D., et al.: Sparse array design for automotive MIMO radar. In: 2019 16th European Radar Conference (EuRAD), pp. 249–252 (2019)
38. Interference in 79 GHz Phase-Coded Automotive Radar. http://resolver.tudelft.nl/uuid:a22d5686-0d83-402b-94cc-4b49c2a63853
39. Boyd, S., Vandenberghe, L.: Convex Optimization. Cambridge university press (2004)
40. Hadjisavvas, N., Komlósi, S., Schaible, S.: Nonconvex Optimization and its Applications (2005). https://doi.org/10.1007/b101428
41. Kirkpatrick, S., Gelatt, C.D., Vecchi, M.P.: Optimization by simulated annealing. Science 220(4598), 671–680 (1983). https://doi.org/10.1126/science.220.4598.671
42. Gourova, R., Pribić, R., Yarovoy, A.: Theory and practice of an Alltop waveform. In: 2016 17th International Radar Symposium (IRS), Krakow, Poland, pp. 1–6 (2016). https://doi.org/10.1109/IRS.2016.7497324
43. Galati, G., Pavan, G.: Waveforms design for modern and MIMO radar. In: Eurocon 2013, Zagreb, Croatia, pp. 508–513 (2013). https://doi.org/10.1109/EUROCON.2013.6625029
44. Giroto de Oliveira, L., et al.: Doppler shift tolerance of typical pseudo-random binary sequences in PMCW radar. Sensors 22(9), 3212 (2022). https://doi.org/10.3390/s22093212
45. Hou, K., Ren, W., Liu, Q.: Majorization minimization based memetic algorithm for designing polyphase sequences with good correlation properties. In: 2019 IEEE International Conference on Signal, Information and Data Processing (ICSIDP), Chongqing, China, pp. 1–6 (2019). https://doi.org/10.1109/ICSIDP47821.2019.9173364
46. Tan, U., et al.: Phase code optimization for coherent MIMO radar via a gradient descent. In: 2016 IEEE Radar Conference (RadarConf), Philadelphia, PA, USA, pp. 1–6 (2016). https://doi.org/10.1109/RADAR.2016.7485178
47. Tan, U., et al.: Optimization methods for solving the low autocorrelation sidelobes problem. In: 2016 17th International Radar Symposium (IRS), Krakow, Poland, pp. 1–5 (2016). https://doi.org/10.1109/IRS.2016.7497323

48. Hu, J., et al.: Designing unimodular waveform(s) for MIMO radar by deep learning method. IEEE Trans. Aero. Electron. Syst. 57(2), 1184–1196 (2021). https://doi.org/10.1109/TAES.2020.3037406
49. Heredia Conde, M., Loffeld, O.: Fast Approximate Construction of Best Complex Antipodal Spherical Codes (2017)
50. Heredia Conde, M., Loffeld, O.: Iterative hard thresholding with optimal measurement matrices. In: 2018 5th International Workshop on Compressed Sensing Applied to Radar, Multimodal Sensing, and Imaging (CoSeRa) (2018). https://www.eurasip.org/Proceedings/Ext/CoSeRa2018/papers/p-herediaconde.pdf
51. Lu, C., Li, H., Lin, Z.: Optimized Projections for Compressed Sensing via Direct Mutual Coherence Minimization (2018). https://arxiv.org/abs/1508.03117
52. Nagesh, S., Ender, J., González-Huici, M.A.: Array position optimisation for compressed sensing MIMO radar based on mutual coherence minimisation. In: 2022 23rd International Radar Symposium (IRS), Gdansk, Poland, pp. 98–103 (2022). https://doi.org/10.23919/IRS54158.2022.9904978
53. Beiker, S.: Deployment scenarios for vehicles with higher-order automation. In: Maurer, M., et al. (eds.) Autonomous Driving. Springer, Berlin (2016). https://doi.org/10.1007/978-3-662-48847-8_10

How to cite this article: Nagesh, S., et al.: Sequence optimisation for compressed sensing CDMA MIMO radar via mutual coherence minimisation. IET Radar Sonar Navig. 18(7), 1178–1192 (2024). https://doi.org/10.1049/rsn2.12555